Optimization of Supercritical CO_2 Power Conversion System With an Integrated Energy Storage for the Pulsed DEMO

Ladislav Vesely, Jan Syblik, Slavomir Entler, Jan Stepanek, Pavel Zacha, and Vaclav Dostal

***Abstract*— DEMO fusion power reactor features multiple different grade heat sources, like the first wall and blanket, divertor, and vacuum vessel. The way of using these sources and their compatibility with the power conversion cycle will affect the efficiency of electricity production. A significant complication is a pulse operation of the fusion reactor unless the noninductive generation of the plasma electric current is developed. In this case, an energy storage application is necessary for conventional electricity production. This article is focused on the supercritical CO_2 power conversion Brayton cycle and on optimization of selected S-CO_2 layouts with the integrated energy storage. The purpose is to compare the efficiency of selected cycle layouts and to find the highest efficiency layout with the multiple different grade heat sources and energy storage.**

***Index Terms*— DEMO, efficiency, energy storage, fusion power plant, power conversion cycle, S-CO_2.**

I. Introduction

THE fusion energy is one of the best way to reduce the emission of CO_2, decrease the price of electricity, and ensure a stable supply of electricity. The research of the fusion energy source and transferring the energy from fusion reaction to thermal and electric energy has been carried out for several decades.

The main goal of the fusion power plant DEMO is to demonstrate the continual electricity production by nuclear fusion. The electricity generation will be performed by a thermodynamic conversion cycle [1]. The research is focused on the steam Rankine or gas Brayton cycles [2], [3]. However, the main problem with the DEMO is the pulsed mode. The pulsed mode cannot prove continuous electricity production by nuclear fusion [4]. One idea, how to eliminate this problem is to combine the thermodynamic conversion cycle with the energy storage system [5], a similar principle used by solar power plants [6], [7].

This research presented in this article will focus on the combination of the thermodynamic conversion cycle with the energy storage system, especially on the supercritical CO_2 power conversion Brayton cycle. The S-CO_2 power cycle is proposed as an alternative to the Rankine cycle. The reason is that the S-CO_2 cycle achieves high efficiency at low operating temperatures [8]. The S-CO_2 cycles are more compact than the water and helium cycles and compressor and turbine are significantly smaller due to the high operating pressures [8], [9].

The results will compare the supercritical CO_2 power conversion Brayton cycle and on optimization of selected S-CO_2 layouts with the integrated energy storage.

II. Technical Parameters of DEMO Fusion Power Plant

DEMO-pulsed fusion reactor has three main thermal heat sources: the first wall and blanket (BNK), divertor (D), and vacuum vessel (VV) with different output temperatures and thermal powers [10]–[12]. The European DEMO reference model is issued in 2015 with the fusion power of 2037 MW and thermal power of 2500 MW. The parameters of the DEMO-pulsed fusion reactor are shown in Table I.

III. Description of Pulsed Mode and Energy Storage

DEMO will operate in pulses of ∼2 h separated by the dwell periods of ∼0.5 h [4]. The pulsed mode is shown in Fig. 1, which describe primary coolant inlet, primary coolant outlet, and secondary steam temperatures, over multiple pulses [4]. According to Fig. 1, the decrease/increase of the temperature of the cooling system is clearly visible. The change in temperature depends on the decrease of thermal power. It is contemplated in this article that the thermal power during the dwell periods will be zero MW and decay heat is neglected.

One idea, how to eliminate this problem, is to combine the thermodynamic conversion cycle with the energy storage system [5]. However, the energy storage system is a very

Manuscript received July 8, 2019; revised November 8, 2019; accepted February 2, 2020. This work was supported in part by the European Regional Development Fund-Project "Center for Advanced Applied Science" under Grant CZ.02.1.01/0.0/0.0/16-019/0000778 and in part by the Strategy AV21 of the Czech Academy of Sciences within the Research Program "Systems for Nuclear Energy." The review of this article was arranged by Senior Editor G. H. Neilson. *(Corresponding author: Ladislav Vesely.)*

Ladislav Vesely is with Czech Technical University in Prague, 166 36 Prague, Czech Republic, and also with the Center for Advanced Turbomachinery and Energy Research (CATER), University of Central Florida, Orlando, FL 32816 USA (e-mail: ladislav.vesely@fs.cvut.cz).

Jan Syblik, Jan Stepanek, Pavel Zacha, and Vaclav Dostal are with Czech Technical University in Prague, 166 36 Prague, Czech Republic.

Slavomir Entler is with Czech Technical University in Prague, 166 36 Prague, Czech Republic, and also with the Institute of Plasma Physics of the CAS, 182 00 Prague, Czech Republic.

Color versions of one or more of the figures in this article are available online at http://ieeexplore.ieee.org.

Digital Object Identifier 10.1109/TPS.2020.2971718

TABLE I
HEAT SOURCES PARAMETERS [13]

First wall and blanket	
Thermal power	2176 MW
Cooling medium	Helium
Pressure	8.00 MPa
Input temperature	300 °C
Output temperature	500 °C
Divertor	
Thermal power	259 MW
Cooling medium	Water
Pressure	5.00 MPa
Input temperature	150 °C
Output temperature	161.5 °C
Vacuum vessel	
Thermal power	65 MW
Cooling medium	Water
Pressure	3.15 MPa
Input temperature	190 °C
Output temperature	200 °C

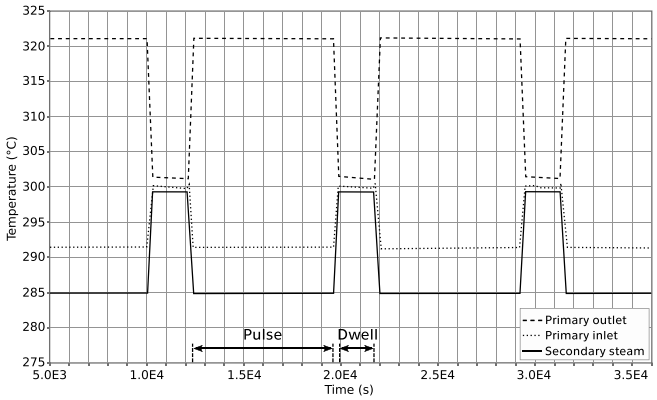

Fig. 1. Description of DEMO Pulsed Mode [4].

complex system, which depends on the source of energy, and time for storage and power [14], [15].

The energy storage can be done by several methods. The basic methods are as follows: mechanical, chemical, electrochemical, and thermal [14], [16]. Each of these methods has some submethods based on different physical/chemical principles. The first question, when it is needed to design the energy storage system, is defined by the amount and time for energy storage. Some methods have the best conditions for short-term storage, for example, chemical storage (batteries). Other methods are developed for long-term storage or for the elimination of the electrical peak. The basic energy storage technologies are pumped hydroelectric storage, based on the gravitational force and pumping water into the reservoir, compressed air storage, based on the principle of compressing air or other gas into the reservoir and gradually pumping it, flywheels based on kinetic energy, sensible heat thermal storage based on aim to heat the working material without changing the volume and pressure, and latent heat thermal storage based on the principle of heat transfer during phase change of operating medium [14]–[16].

The total power in the DEMO-pulsed Fusion reactor is 2500 MW (see Table I). The pulse period is 2 h and the dwell period is 30 min. For this reason, it is necessary to store approximately 1/5 of power for 2 h. This is a large amount of energy which has to be stored. However, storage is only necessary for the short term. The energy storage with acceptable parameters for this application could be based on a thermal method. The thermal method uses two principles, the sensible heat storage and the latent heat storage [15]. The latent heat storage seems to be the best way for combining the thermodynamic conversion cycle with the energy storage system [5].

The latent heat storage uses molten salts which are placed in low- and high-temperature tanks [5], [15], [16]. The heat is transferred via heat exchangers, which can be easily connected with S-CO_2 power cycle. On the other hand, the DEMO-pulsed fusion reactor does not need electric plasma heating during the dwell period for maintaining plasma. This power can be used for heating up in the dwell period. This reduces the demand on energy storage [13].

IV. DESCRIPTION OF CYCLE LAYOUTS FOR NORMAL AND PULSED MODE

The investigated cycle is the Brayton cycle which uses the S-CO_2 as the working medium. The S-CO_2 power cycle is one of the investigated power cycle for transformation energy from fusion reactor to electricity [8], [17], [18]. The S-CO_2 power cycle is proposed as an alternative to the Rankine cycle, because the S-CO_2 power cycle achieves high efficiency at low operating temperatures [8]. The S-CO_2 power cycles are also more compact than the water and helium cycles and compressor and turbine are significantly smaller due to, the high operating pressures [8], [9].

The basic Brayton cycle consists of a compressor, a turbine, a cooler, and a heat source. To improve the cycle efficiency the cycles use recuperative heat exchanger [9], [19]. The basic layout of the S-CO_2 power cycle is the simple Brayton cycle (see Fig. 2). The simple Brayton S-CO_2 power cycle in Fig. 2 is modified for the fusion application with energy storage units in the burn period.

The simple Brayton S-CO_2 power cycle consists of the compressor, the turbine, the cooler, two recuperative heat exchangers (LTR and HTR), three heat sources (D—divertor, VV—vacuum vessel, and B—first wall and blanket), and three energy storage utilities (DES—divertor energy storage, VVES—vacuum vessel energy storage, BES—first wall and blanket energy storage). The heat sources and energy storage utilities are connected on the same line. This line is connected with the S-CO_2 power cycle via three heaters (DE—divertor heat exchanger, VVE—vacuum vessel heat exchanger and BE—first wall and blanket heat exchanger).

The layout for the simple Brayton S-CO_2 power cycle in the dwell period is shown in Fig. 3. The cycle consists of the same components as the simple Brayton S-CO_2 power cycle in the burn period. However, the cycle layout for the dwell period is improved with an electric heater (EH) (see Fig. 3). The power which is considered in EH is the power that is necessary to maintain the plasma. This power can be used in the dwell period because plasma heating is not necessary in the dwell period. The power is approximately 200 MW [13].

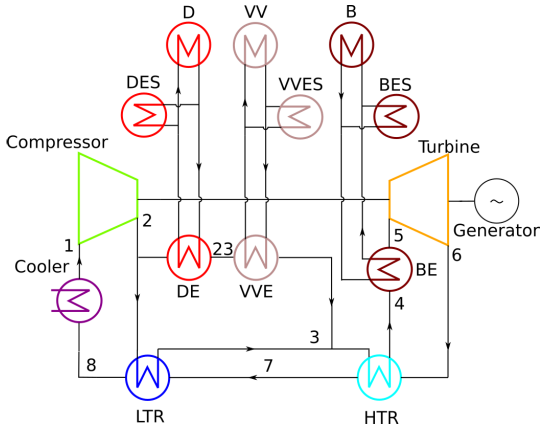

Fig. 2. Simple Brayton S-CO_2 cycle—pulse period.

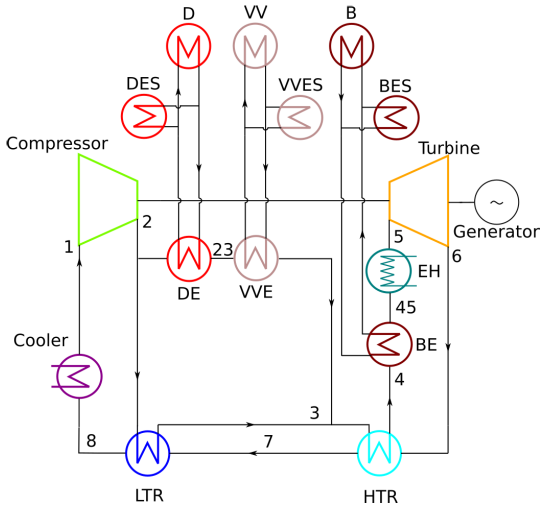

Fig. 3. Simple Brayton S-CO_2 cycle—dwell period.

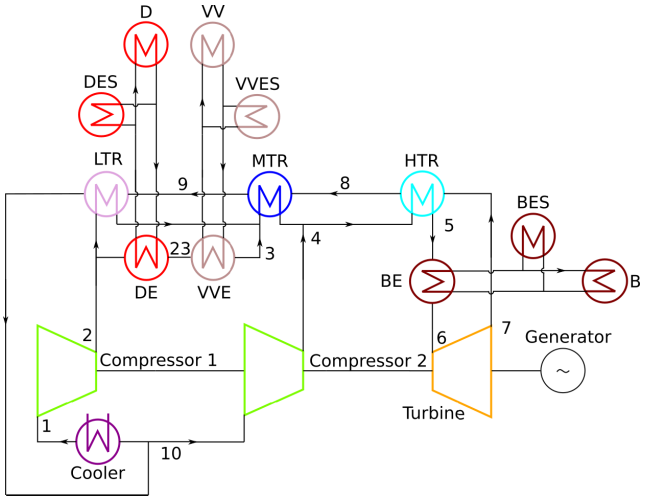

Fig. 4. Re-compression S-CO_2 cycle—burn period.

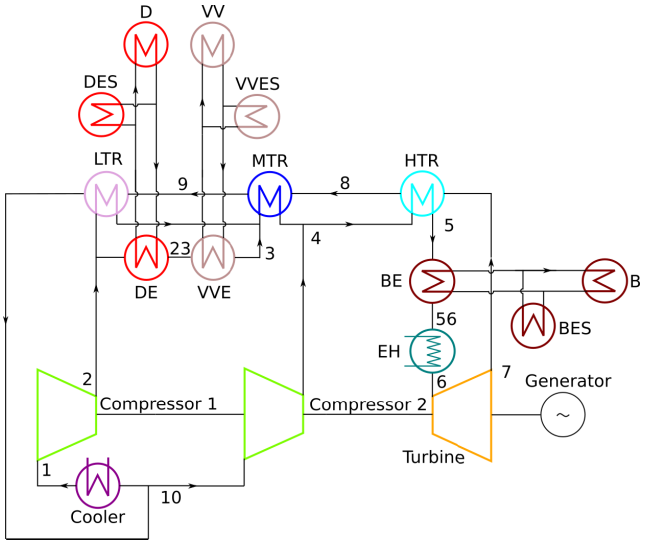

Fig. 5. Recompression S-CO_2 cycle—dwell period.

Another S-CO_2 power cycle is the recompression S-CO_2 power cycle (see in Fig. 4). The recompression S-CO_2 power cycle consists of two compressors, the turbine, the cooler, three recuperative heat exchangers (LTR, MTR, and HTR), three heat sources (D—divertor, VV—vacuum vessel, and B—first wall and blanket), three energy storage utilities (DES—divertor energy storage, VVES—vacuum vessel energy storage, BES—first wall and blanket energy storage), and three heaters (DE—divertor heat exchanger, VVE—vacuum vessel heat exchanger, and BE—first wall and blanket heat exchanger).

The difference between the simple Brayton cycle and the recompression cycle is in the additional compressor. The recompression cycle is more complex. The main difference or benefit lies in dividing the flow before cooling into two streams. One stream goes through the cooler to the main compressor, and the second stream goes through the recompressor. The recompression S-CO_2 power cycle in Fig. 4 is modified for the fusion application with energy storage units in the burn period.

The layout for the recompression S-CO_2 power cycle in the dwell period is shown in Fig. 5. The cycle consists of the same components as the recompression S-CO_2 power cycle in the burn period. However, the cycle layout for the dwell period is improved with EH, powered by the unused power for plasma heating, as the simple Brayton S-CO_2 power cycle in the dwell period (see Figs. 3 and 5).

V. Description of Optimization

The optimization was done in cooling cycles optimization computational software (CCOCS). This software is based on experience from previous research [20]–[22], and it was extended in order to compute the energy storage system. The thermodynamical values are gained from CoolProp C++ thermodynamic libraries [23]. At the same time, the NIST Reference Fluid Thermodynamic and Transport Properties database, Version 9.1 [24] was used.

The efficiencies of the cycle devices are given in Table II.

The boundary conditions of the computational model are based on efficiencies of the heat exchangers and on minimal temperature differences. The efficiency of the heat exchanger

TABLE II
EFFICIENCIES OF THE CYCLE DEVICES

Compressor efficiency η_C	89 %
Turbine efficiency η_T	90 %
Pressure efficiency in heat exchangers η_{PH}	98 %
Pressure efficiency in cooler η_{PC}	95 %
Electrical heating efficiency η_{EH}	90 %
Energy storage efficiency η_{ES}	95 %

has to be lower than 95% and the minimum temperature difference has to be higher than 5 °C. The initial input values are compressor inlet pressure p_1, compressor outlet pressure p_2, the temperature difference between compressor outlet temperature and cooler inlet temperature Δth, thermal energy that is not stored from divertor PD, and thermal energy that is not stored from the vacuum vessel.

The minimum temperature difference is computed in the whole heat exchanger. This validation has to be done because of the possible negative temperature in pinch point [25].

There are two modes of calculation. The first mode of calculation is by using part of the energy from all heat sources and the rest is stored to the energy storage (burn period). This mode lasts approximately two hours, and after this period the energy sources are turned off. After the input of the values, how much energy the cooling cycle needs to get from the high potential source is calculated (first wall and blanket). The calculation is done in order to get the same net power in the first and second modes. For this specific layout, it is necessary to have the power at around 1960 MW.

The second mode lasts approximately 30 min (dwell period). The only energy which is transferred to the cooling cycle is the energy from the energy storage. It is also necessary to use the energy which is reserved for plasma heating. This source has 200 MW and in order to preserve the constant net power, this energy source is used for electric heating of the cooling system (between points 45 and 5 for Simple Brayton cycle and between 56 and 6 for Recompression cycle in Figs. 3 and 5).

The initial conditions for the second mode are constant net power, as was mentioned, constant admission and emission pressure in the turbine and equal mass flow in the turbine.

The optimal result is the one that gains the highest total efficiency. For one input, two efficiencies for both modes are computed and from these two values the total efficiency is computed. The variation of the input values are saved, and the final output files are generated and plotted to obtain the result.

The optimization method is described in Fig. 6.

The optimization code COCOS was written for optimization of the S-CO_2 power cycles with additional heat sources (DE, VVE, and BE). The boundary conditions for the storage systems are inlet/outlet temperature and mass flow in the DE, VVE, and BE.

VI. RESULTS

Calculation was performed according to Fig. 6 with parameters in Table II. The compressor inlet temperature is 34 °C, the turbine inlet temperature is 480 °C.

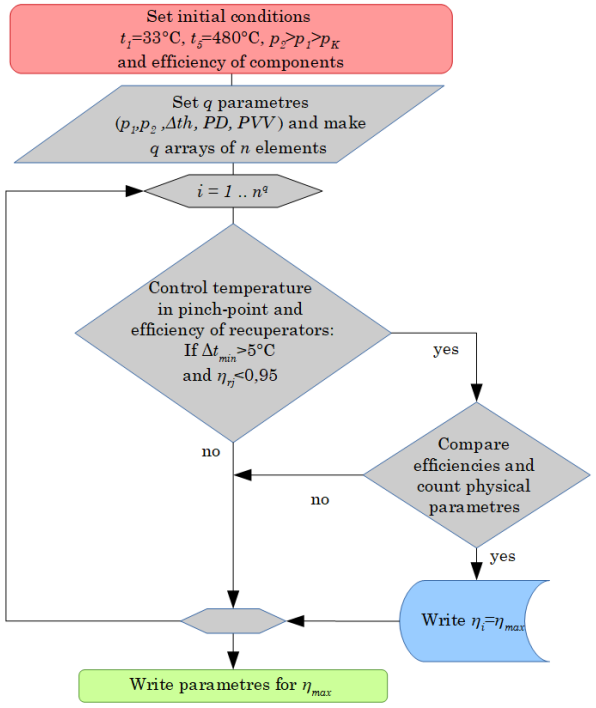

Fig. 6. Scheme of optimization software.

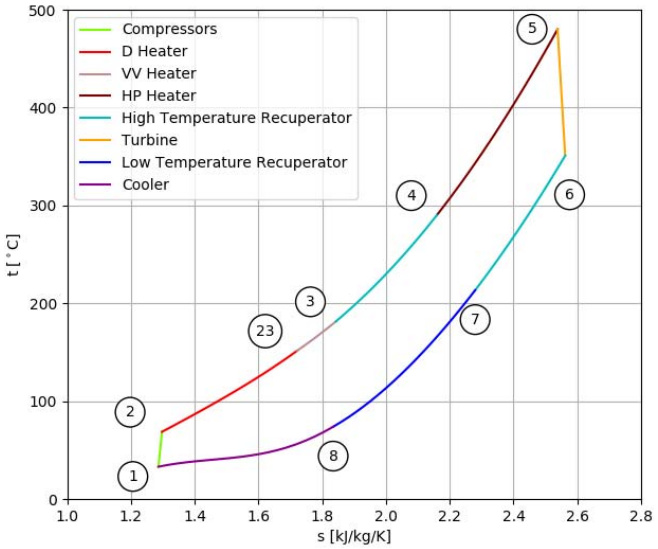

Fig. 7. T-S diagram of the simple Brayton S-CO_2 cycle—burn period.

T-S diagram for the simple Brayton S-CO_2 power cycle in the burn period and the dwell period is shown in Figs. 7 and 8, respectively. The results are very similar for both periods. The dwell period will not produce any effect on the continued production of electricity.

The boundary conditions for optimization are constant turbine power for the pulse and dwell period. The turbine power for the simple Brayton S-CO_2 power cycle is 947 MW, the compressor input power is 250 MW and the net power is 697 MW (see Tables III and IV). The mass flow rate is

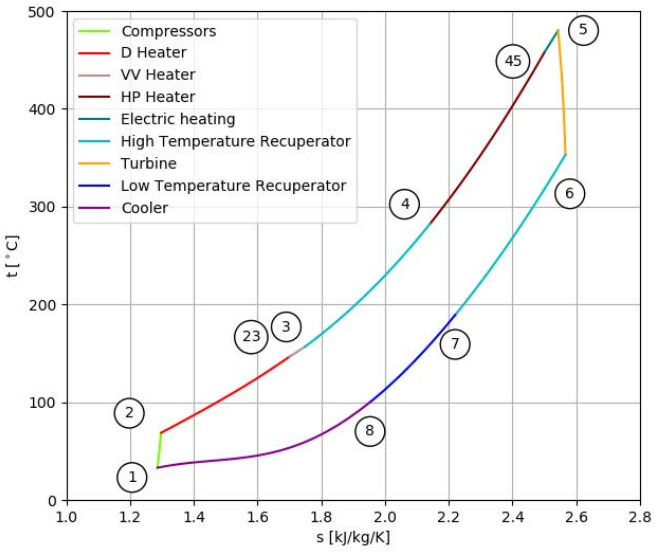

Fig. 8. T-S diagram of the simple Brayton S-CO_2 cycle—dwell period.

TABLE III
RESULTS FOR BURN PERIOD

	Simple	Re-Compression	
Turbine inlet pressure	30.4	32.4	MPa
Mass flow rate	7145	8231	kg/s
Turbine power output	947	1122	MW
Compressor power input	250	388	
Added heat	1960	1960	
Removed heat	1263	1227	
Net power	**697**	**734**	**MW**
Cycle efficiency	**35.6**	**37.4**	**%**

the same for both periods, i.e., 7145 kg/s. The turbine inlet pressure was optimized at 30.4 MPa. Due to the same flow and pressure, the cycle gets the same turbine power output and net power. However, the cycle efficiency is 35.6% for the burn period and only 30.3% for the dwell period.

The results in Table III are for the simple Brayton S-CO_2 power cycle and the recompression S-CO_2 power cycle in the burn period. Table IV shows the results for the simple Brayton S-CO_2 power cycle and the recompression S-CO_2 power cycle in the dwell period.

The recompression S-CO_2 power cycle has the turbine power output 1122 MW, the compressor input power is 388 MW, the mass flow rate is 8231 kg/s, and net power is 734 MW for the burn period. The net power for the recompression S-CO_2 power cycle in the dwell period is 750 MW. An increase in net power can be observed. The increase in the net power is achieved by reducing compression input power due to a change in flow distribution in the streams (see Figs. 9 and 10). The compressor input power is 372 MW for the dwell period (see Table IV).

The cycle efficiency is 37.4% for the burn period and 33.3% for the dwell period. The T–S diagram for the recompression S-CO_2 power cycle in the burn period and the dwell period is shown in Figs. 9 and 10, respectively.

TABLE IV
RESULTS FOR DWELL PERIOD

	Simple	Re-Compression	
Turbine inlet pressure	29.8	32.4	MPa
Mass flow rate	7145	8231	kg/s
Turbine power output	932	1122	MW
Compressor power input	250	372	
Added heat	2250	2250	
Removed heat	1568	1500	
Net power	**682**	**750**	**MW**
Cycle efficiency	**30.3**	**33.3**	**%**

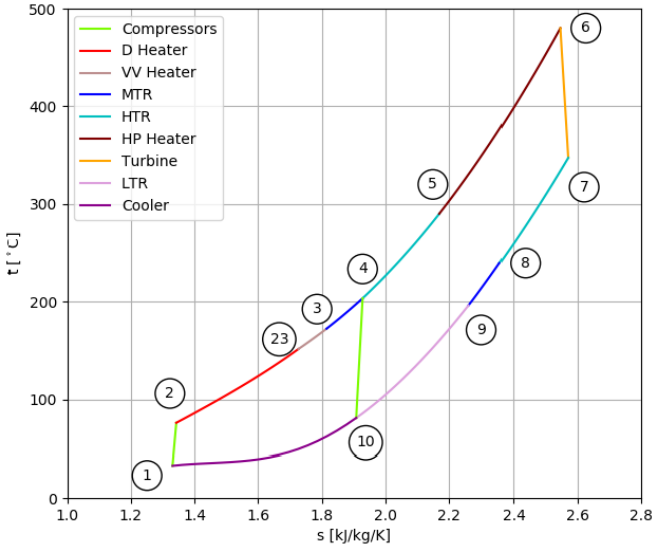

Fig. 9. T-S diagram of the recompression S-CO_2 cycle—burn period.

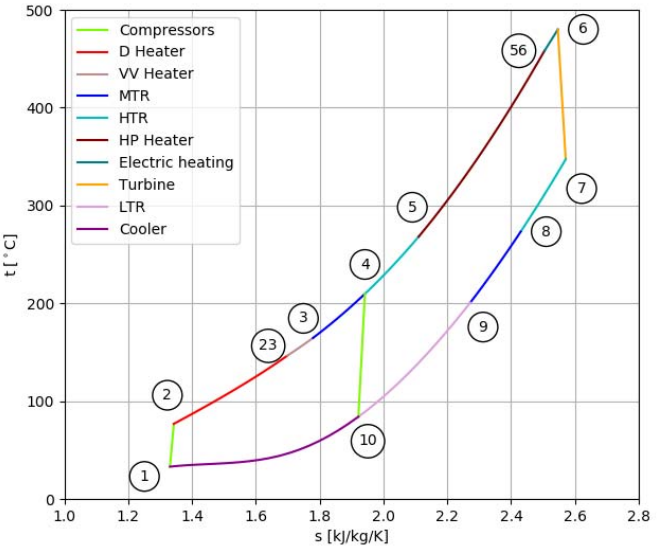

Fig. 10. T-S diagram of the recompression S-CO_2 cycle—dwell period.

The optimization shows the layout of storage power. The total heat power which is used for conversion of heat to electrical power is 1960 MW (see Tables III and V). The thermal power for storage systems is 540 MW for both cycle layouts. It is obvious that around 22% of thermal power has

TABLE V
DISTRIBUTION OF THERMAL POWER BETWEEN AN ELECTRICITY PRODUCTION AND STORAGE IN BURN PERIOD

	Simple	**Re-Compression**	
Burn period - electricity production			
Vacum vessel	52	45	MW
Divertor	160	154	
First wall and Blanket	1748	1761	
Thermal power - Pulse mode	**1960**	**1960**	**MW**
Burn period - storaged power			
Vaccum vessel	13	20	MW
Divertor	99	105	
First wall and Blanket	428	415	
Thermal power - Storage	**540**	**540**	**MW**

to be stored during the burn period in order to gain the same amount of electric power in the electric network.

The storage system for the simple Brayton S-CO_2 power cycle uses thermal power from the divertor, vacuum vessel, and first wall and blanket. The lowest thermal power is used from the vacuum vessel for storage in this cycle layout. The storage system for the recompression S-CO_2 power cycle also uses the thermal power from three sources. However, according to Table V, the storage system uses 31% of the total thermal power from the vacuum vessel in the case of the recompression cycle and only 20 % in a simple Brayton cycle layout.

VII. CONCLUSION

The idea of the combination of the thermodynamic conversion cycle with the energy storage system, especially on the supercritical CO_2 power cycle, can be realistically implemented in the design of the DEMO-pulsed fusion power plant with pulse mode. The continuous electricity production can be provided, as shown in the results. The net power investigated for both power cycles and for both periods (pulse and dwell) is the same or slightly increased, which can be used for self-consumption power in the dwell period.

The amount of energy, which has to be stored, is huge for the dwell period. The results showed that thermal energy is stored according to the cycle layout. The thermal power may not be stored from all sources equally, for example, the optimization method lowers the amount of energy stored from the vacuum vessel. Hence, the design of the different storage systems for each heat source is an interesting clue as to how we can eliminate the size and reduce the price of storage systems. The optimization method used parameters such as the boundary conditions for the storage systems, inlet/outlet temperature, and mass flow in the DE, VVE, and BE, respectively. This method is very useful for optimization if the exact way to store energy is not known.

The optimization method concluded that the recompression cycle gains higher efficiency, which is about 2% higher in the burn period and about 3% higher in the dwell period. The simple Brayton cycle used the lower part of energy production from the vacuum vessel and higher part of energy from the divertor.

REFERENCES

[1] J. L. Linares *et al.*, "Brayton power cycles for electricity generation from fusion reactors," *J. Energy Power Eng.*, vol. 5, pp. 590–599, Jul. 2011.

[2] M. Medrano *et al.*, "Power conversion cycles study for He-cooled reactor concepts for DEMO," *Fusion Eng. Des.*, vol. 82, nos. 15–24, pp. 2689–2695, Oct. 2007.

[3] L. Vesely, V. Dostal, and S. Entler, "Comparison of supercritical CO_2 power cycles for nuclear energy," in *Proc. Acta Polytechnica CTU*, vol. 4, 2016, p. 6, doi: 10.14311/AP.2016.4.0107.

[4] C. Harrington, "Dynamic modelling of balance of plant systems for a pulsed DEMO power plant," *Fusion Eng. Design*, vols. 98–99, pp. 2147–2151, Oct. 2015, doi: 10.1016/j.fusengdes.2015.03.029.

[5] J. Lucas, M. Cortes, P. P. Mendez, J. Hayward, and D. Maisonnier, "Energy storage system for a pulsed DEMO," *Fusion Eng. Des.*, vol. 82, pp. 2752–2757, Oct. 2007, doi: 10.1016/j.fusengdes.2007.03.007.

[6] M. Zhiwen and C. S. Turchi, "Advanced supercritical carbon dioxide power cycle configurations for use in concentrating solar power systems," NREL, Golden, CO, USA, Tech. Rep. NREL/CP-5500-50787, 2011.

[7] B. D. Iverson, T. M. Conboy, J. J. Pasch, and A. M. Kruizenga, "Supercritical CO_2 brayton cycles for solar-thermal energy," *Appl. Energy*, vol. 111, pp. 957–970, Nov. 2013.

[8] L. Vesely, V. Dostal, and S. Entler, "Study of the cooling systems with S-CO_2 for the DEMO fusion power reactor," *Fusion Eng. Des.*, vol. 124, pp. 244–247, Nov. 2017, doi: 10.1016/j.fusengdes.2017.05.029.

[9] K. Brun, P. Friedman, and R. Dennis, *Fundamentals and Applications of Supercritical Carbon Dioxide (S-CO_2) Based Power Cycles*. Amsterdam, The Netherlands: Elsevier, 2016.

[10] L. V. Boccaccini *et al.*, "Objectives and status of EUROfusion DEMO blanket studies," *Fusion Eng. Des.*, vols. 109–111, pp. 1199–1206, Nov. 2016.

[11] J. H. J. H. You *et al.*, "Conceptual design studies for the European DEMO divertor: Rationale and first results," *Fusion Eng. Des.*, vols. 109–111, pp. 1598–1603, Nov. 2016.

[12] G. Federici *et al.*, "Overview of EU DEMO design and R&D activities," *Fusion Eng. Des.*, vol. 89, pp. 882–889, Oct. 2014.

[13] C. Bachmann *et al.*, "Issues and strategies for DEMO in-vessel component integration," *Fusion Eng. Des.*, vol. 2016, vol. 112, pp. 527–534, Nov. 2016.

[14] T. Letcher, *Storing Energy With Special Reference to Renewable Energy Sources*. Amsterdam, The Netherlands: Elsevier, 2016.

[15] I. Dincer and M. A. Rosen, *Thermal Energy Storage Systems and Applications*. Hoboken, NJ, USA: Wiley, 2011.

[16] T. Kousksou, P. Bruel, A. Jamil, T. El Rhafiki, and Y. Zeraouli, "Energy storage: Applications and challenges," *Sol. Energy Mater. Sol. Cells*, vol. 120, pp. 59–80, Jan. 2014, doi: 10.1016/j.solmat.2013.08.015.

[17] J. I. Linares, A. Cantizano, B. Y. Moratilla, V. Martín-Palacios, and L. Batet, "Supercritical CO_2 brayton power cycles for DEMO (demonstration power plant) fusion reactor based on dual coolant lithium lead blanket," *Energy*, vol. 98, pp. 271–283, Mar. 2016.

[18] J. L. Linares *et al.*, "Supercritical CO_2 brayton power cycles for DEMO fusion reactor based on helium cooled lithium lead blanket," *Appl. Therm. Eng.*, vol. 76, pp. 123–133, Feb. 2015, doi: 10.1016/j.applthermaleng.2014.10.093.

[19] G. Angelino, "Carbon dioxide condensation cycles for power production," *J. Eng. Power*, vol. 90, no. 3, pp. 287–295, 1968, doi: 10.1115/1.3609190.

[20] J. Syblik, L. Vesely, S. Entler, J. Stepanek, and V. Dostal, "Analysis of supercritical CO_2 brayton power cycles in nuclear and fusion energy," *Fusion Eng. Des.*, vol. 146, pp. 1520–1523, Sep. 2019, doi: 10.1016/j.fusengdes.2019.02.119.

[21] J. Stepanek, L. Vesely, and V. Dostal. (2016). *Supercritical Carbon Dioxide Heat Cycle Optimization Code*. [Online]. Available: http://energetika.cvut.cz/RIV/software

[22] L. Vesely, "Study of power cycle with supercritical CO_2," Dept. Energy Eng., Czech Tech. Univ. Prague, Prague, Czechia, Tech. Rep., 2018.

[23] I. Bell. (2017). *Bell, I.CoolProp: An Open-source Thermophysical Property Library*. Accessed: Jul. 30, 2018. [Online]. Available: http://coolprop.sf.net

[24] E. W. Lemmon, M. L. Huber, and M. O. McLinden, *NIST Standard Reference Database 23: Reference Fluid Thermodynamic and Transport Properties-REFPROP, Version 9.1*, Standard Reference Data Program, National Institute of Standards and Technology, Gaithersburg, MD, USA, 2013.

[25] L. Vesely, V. Dostal, O. Bartos, and V. Novotny, "Pinch point analysis of heat exchangers for supercritical carbon dioxide with gaseous admixtures in CCS systems," *Energy Procedia*, vol. 86, pp. 489–499, Jan. 2016, doi: 10.1016/j.egypro.2016.01.050.